THE JOURNAL OF PHYSICAL CHEMISTRY B

Article

pubs.acs.org/JPCB

Two-Photon Absorption Properties of Chromophores in Micelles: Electrostatic Interactions

Semere Bairu and Guda Ramakrishna*

Department of Chemistry, Western Michigan University, Kalamazoo, Michigan 49008, United States

Supporting Information

ABSTRACT: Two-photon absorption (2PA) cross sections of neutral Coumarin 485 (C485) and anionic Coumarin 519 ($C519^-$) solubilized in Triton X-100 (Tx-100, neutral), sodium dodecyl sulfate (SDS, anionic), and cetyltrimethylammonium bromide (CTAB, cationic) are reported. The objective of the study is to probe the influence of local electrostatic fields in micelles on the 2PA properties of chromophores. The 2PA measurements have shown that the cross sections of neutral C485 are unchanged in different micellar environments, although the local micropolarities of chromophores are different. On the other hand, the 2PA cross sections of $C519^-$ are unchanged or slightly decreased in Tx-100 and SDS micelles when compared to water while 100% increase in 2PA cross sections was observed for $C519^-$ in CTAB micelles. The enhancement in 2PA cross section is attributed to the electrostatic fields arising in the Stern layer of CTAB, where $C519^-$ is solubilized. The titration measurements have shown that the 2PA enhancement is due to the organized medium only and not because of the simple association of $C519^-$ and the quaternary ammonium group of CTAB. From the analysis, local electric field of 0.7 ± 0.3 MV/cm is estimated for the Stern layer of CTAB.

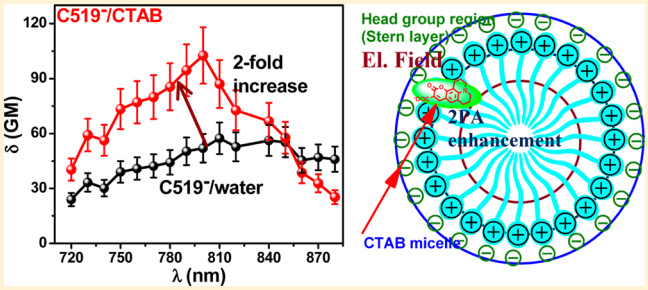

1. INTRODUCTION

Materials with large two-photon absorption (2PA) cross sections have found applications in interdisciplinary areas of sciences that include two-photon microscopy and imaging,[1−3] 3D micro/nano fabrication,[4−6] 3D optical data storage,[7] optical limiting,[8−10] photodynamic therapy,[11,12] TP sensing,[13−15] and biophysics.[16,17] For all these applications, chromophores with large 2PA cross sections are necessary. Thus, most of the research is focused on designing better and efficient 2PA materials. Several organic chromophores with dipolar, quadrupolar, octupolar, and dendritic architectures[18−25] were designed and synthesized to achieve better 2PA cross sections with great success. Although enormous research is focused on developing better 2PA materials, little is known about the influence of environment on the 2PA cross sections of the chromophores. Solvent polarity, microheterogeneous media, and confined geometries tend to influence the optical properties of chromophores like fluorescence quantum yields, electron-transfer reactions, photostability, solvation dynamics, etc.[26−38]

Recent literature has focused on probing the effect of solvent polarity on 2PA cross sections.[39−46] Agren and co-workers[46] have theoretically shown that the influence of the solvent polarity on the 2PA cross sections is not significant. Bazan and co-workers[39] have studied the solvent effect on the 2PA properties of D-π-A-π-D chromophores and shown that the influence of solvent polarity on the 2PA cross sections is quite nonmonotonic and maximum 2PA cross section is observed in solvents of intermediate polarity. Theoretical approaches have focused on explaining this trend and were quite successful.[38,46] However, the reports probing the effect of microheterogeneous environment on the 2PA cross sections of chromophores are sparse.[47−51] Bazan and co-workers have studied the 2PA properties of paracyclophane derivatives in aqueous micellar solutions and have shown large enhancements in 2PA cross sections.[47] But, the enhancement was attributed to solvent polarity rather than the organized assembly. A recent report has focused on the 2PA cross sections of quadrupolar chromophores in cyclodextrins and they have observed 2- to 3-fold increase in the 2PA cross sections of chromophores in cyclodextrins.[52] However, there are no systematic reports probing the micellar environment on the 2PA cross sections of chromophores with intramolecular charge-transfer character. Micelles, by virtue of the chemical composition of the surfactants that form them, can be cationic, neutral, and anionic. It will be interesting to probe how these different micellar environments can influence the 2PA cross sections of chromophores solubilized in them.

Thus, the main goal of the present investigation is to study the influence of micelle environment on the 2PA cross sections of coumarin dye molecules and probe if the electrostatic interactions play a role in altering their cross sections. To

Received: June 1, 2013
Revised: August 6, 2013
Published: August 16, 2013

dx.doi.org/10.1021/jp405416d | J. Phys. Chem. B 2013, 117, 10484−10491

achieve the objective, we have studied the 2PA cross sections of two coumarin dye molecules, C485 (neutral) and C519$^-$ (structures shown in Chart 1) in three different surfactants:

Chart 1. Molecular Structures of the Investigated Chromophores

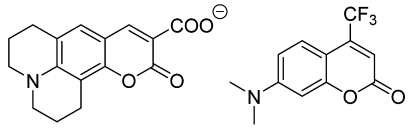

C519$^-$ C485

sodium dodecyl sulfate (SDS, anionic), Triton X-100 (Tx-100, neutral), and cetyltrimethylammonium bromide (CTAB, cationic). The results obtained from the study will shed light on the influence of microheterogeneous environment on the 2PA cross sections of chromophores.

2. EXPERIMENTAL SECTION

2.1. Materials. SDS, Tx-100, and CTAB were obtained from Sigma-Aldrich and were used as received. Milipore water was used to make the aqueous solutions of micelles. The dye molecules C519 and C485 were purchased from Exciton Inc. All the measurements of absorption, fluorescence, two-photon cross section, and time-resolved measurements were performed in surfactant concentrations of at least 2 times above the critical micelle concnetration (cmc) of the repsective micelles unless stated otherwise. Anionic C519 was prepared by adopting a published procedure[53] with a small modification where methanol was used instead of water for efficient removal of the solvent. Briefly, the sodium salt of C519 (C519$^-$) was prepared by dissolving C519 in methanol and increasing the pH of solution to 10 using NaOH and the salt of C519 was obtained by rotary evaporating methanol. The absorption and fluorescence spectra of C519$^-$ matched quite well with the published spectra.[53]

2.2. Methods. Optical absorption measurements were carried out in a Shimadzu UV-2101PC spectrophotometer and steady-state fluorescence measurements were carried out in an Edinburgh spectrofluorimeter. All the optical measurements were carried out in quartz cuvettes of 0.4 cm path lengths. The quantum yields of the dye molecules in various media were measured using C485 in methanol as the standard.[54] We have used the same refractive index as that of water for the dyes inside micelles for fluorescence quantum yield measurements.

To measure the 2PA cross sections, two-photon-excited fluorescence (2PEF) technique was employed.[55,56] A 10^{-4} M C485 solution in methanol was used as a reference over a wavelength range of 720−900 nm with the cross sections of the standard reported earlier.[56] The concentrations of chromophores in micelles was kept at 10^{-5} M so that the same samples can be used for both one-photon fluorescence quantum yield and two-photon fluorescence measurements. The concentrations of micelles are kept at 2.5 times of their respective cmc. As the samples have absorption of around 10^{-5} M, the self-absorption is not an issue for both one- and two-photon fluorescence measurements. For the two-photon fluorescence measurements, output from a broadband Ti:sapphire oscillator (SpectraPhysics) was focused onto the sample and the fluorescence was monitored in the Edinburgh spectrofluorimeter. The focal point of the laser on the sample is around 60 μm. The power was varied with a neutral-density filter. All the samples have shown slope 2 power dependence (see Supporting Information) confirming that the fluorescence is indeed arising out of a 2PA event.

The time-resolved fluorescence measurements were studied using the femtosecond fluorescence up-conversion technique described elsewhere.[57] Briefly, the studies were carried out with the second harmonic (400 nm) of the fundamental Ti:sapphire laser at 800 nm, as the excitation source and the upconversion optics from CDP Instruments Inc., Russia. Polarization of the excitation beam was controlled using a Berek compensator, and the sample was continuously rotated with a rotating cell of 1 mm thickness. Polarized fluorescence emitted from the sample was up-converted in a nonlinear crystal of β-barium borate using the gate beam at 800 nm, which first passed through a variable delay line. The instrument response function (IRF) was measured by monitoring the Raman scattering from water. Fitting the Gaussian peak from the Raman scattering yielded a sigma value of ~120 fs which gave a full width half-maximum (fwhm) of ~280 fs. Spectral resolution was achieved using a double monochromator and photomultiplier tube. The excitation average power was mostly in the range of 3.5 ± 0.2 mW.

Fluorescence anisotropy is calculated from the traces obtained after parallel (I_{par}) and perpendicular (I_{per}) excitation with the following equation[58] which is based on the ratio of difference between parallel and perpendicular polarized emissions over magic-angle fluorescence.

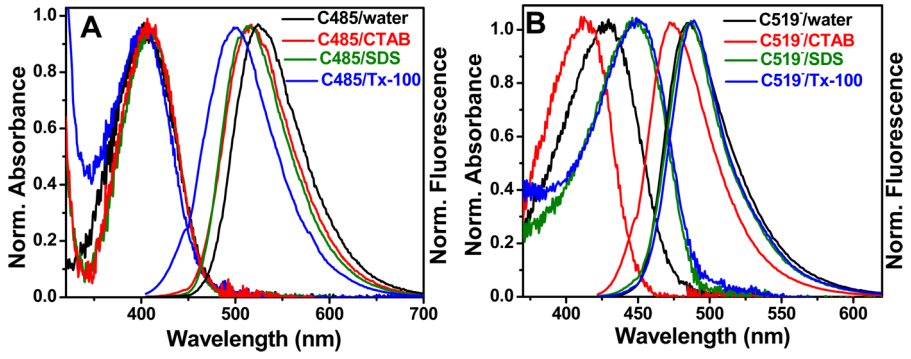

Figure 1. Normalized absorption and fluorescence spectra of 10^{-5} M (A) C485 in water, SDS, CTAB, and Tx-100 and (B) C519$^-$ in water, SDS, CTAB, and Tx-100.

dx.doi.org/10.1021/jp405416d | J. Phys. Chem. B 2013, 117, 10484−10491

$$r(t) = \frac{I_{par}(t) - GI_{per}(t)}{I_{par}(t) + 2GI_{per}(t)} \quad (1)$$

where the G factor accounts for the differences in sensitivities for the detection of emission in perpendicular and parallel polarized configurations. The G factor was obtained from the tail-fitting of the anisotropy decays of perylene in methanol and Coumarin 515 in methanol.

Fluorescence lifetimes in nanosecond time domain were measured using the time-correlated single-photon-counting technique (Edinburgh F900) using a 370 nm diode laser (PicoQuant inc.) as the excitation source. The resultant fluorescence was detected with a cooled Hamamatsu R928P photomultiplier tube. Scattering from aluminum foil was used to obtain the instrument response function (IRF). The fluorescence lifetimes were obtained from deconvoluting the fluorescence decay with IRF.

3. RESULTS AND DISCUSSION

3.1. Steady-State Measurements. Optical absorption and steady-state fluorescence measurements were carried out to study the electronic interactions of chromophores with micelles. The normalized absorption and fluorescence spectra are shown in parts A and B of Figure 1 for C485 and C519$^-$, respectively. The absorption maximum of C485 in different media (water, CTAB, SDS, and Tx-100) was unchanged while the fluorescence maxima shifted to shorter wavelengths with respect to water (Figure 1A). The results indicate that C485 is solublized in the micelles, probably in the palisade layer or the core. From the fluorescence maxima of C485 in different micelles (Table 1), micropolarity where C485 is localized was obtained (see Supporting Information). It is observed that C485 is solublized in the palisade layer (probably little closer to the headgroup) of SDS and CTAB (with a polarity similar to that of methanol) while it was farther from the headgroup in Tx-100 (micropolarity similar to isopropanol). Also, the fluorescence quantum yields of C485 increased significantly when it was bound to the micelles (Table 1).

Table 1. Absorption and Fluorescence Spectral Properties of the Investigated Chromophores in Various Media

sample	λ_{abs}^{max} (nm)	λ_{em}^{max} (nm)	quantum yield (η)	lifetimes
C485/ water	403	524	0.06	[a] τ_1 = 3.5 ps (24.3%), τ_2 = 480 ps (62.4%), τ_3 = 4.7 ns[b] (13.3%)
C485/ CTAB	408	516	0.10	τ_1 = 15.5 ps (5.3%), τ_2 = 450 ps (78.3%), τ_3 = 3.9 ns[b] (16.4%)
C485/ SDS	409	514	0.17	τ_1 = 7.3 ps (10.7%), τ_2 = 480 ps (82%), τ_3 = 4.7 ns[b] (7.4%)
C485/ Tx-100	404	498	0.30	τ_1 = 480 ps (93.5%), τ_2 = 2.8 ns[b] (6.5%)
C519$^-$/ water	431	485	0.70	τ = 4.3[b] ns
C519$^-$/ CTAB	411	474	0.60	τ = 4.4[b] ns
C519$^-$/ SDS	447	486	0.84	τ = 4.3[b] ns
C519$^-$/ Tx-100	449	488	0.56	τ = 4.2[b] ns

[a]Lifetimes for C485 were obtained in methanol as the solubility in water is only about 10 μM. [b]Lifetimes obtained from single-photon-counting technique.

In contrast, the absorption maxima of C519$^-$ varied in different media. The absorption maximum of C519$^-$ is shifted to 447 nm in SDS and 449 nm in Tx-100 micelles while it is shifted to higher energies to 411 nm in CTAB (Figure 1B and Table 1). The results show that C519$^-$ is solubilized in these micelles but CTAB offers different stabilization compared to SDS and Tx-100, which can be attributed to the electrostatic interactions between C519$^-$ and CTAB. Further femtosecond fluorescence lifetime and anisotropy measurements were carried out to confirm the localization of chromophores inside the micelles.

3.2. Time-Resolved Fluorescence Measurements. The fluorescence kinetic decay traces of C485 in different media and corresponding anisotropy traces are shown in parts A and B of Figure 2, respectively. The excited-state relaxation of C485 is mostly dominated by solvation followed by the singlet state relaxation decay (Figure 2A). The fluorescence lifetime of C485 in methanol was fitted with a three-exponential function with lifetimes of 3.5 ps, 480 ps, and 4.7 ns. The 3.5 ps lifetime can be attributed to the solvation time constant of methanol.[54,59] The other two components are attributed to the singlet-state lifetimes. Two lifetime components for the singlet state can be assigned to the presence of a twisted ICT state, which decays nonradiatively. However, the average singlet-state lifetime of C485 matched quite well with that of literature reports.[59] However, when C485 is solubilized in micelles, the solvation component is altered.[30] In Tx-100, the relaxation of C485 is dominated by the ICT state's decay where the solvation component is significantly different than other micelles or to that of methanol. This can be because of different micropolarities in micelles where the chromophore is localized. The anisotropy decays of C485 in different micelles (Figure 2B) show that the anisotropy is longer in the micelles, suggesting that C485 is localized in the micelles, probably in the palisade layer. The anisotropy decay of chromophores in micelles is normally modeled by wobbling in a cone mode with short and long components of the decay.[60] The anisotropy decay traces of C485 in micelles also follow similar wobbling in a cone model with two different decay components. In addition, the fact that there is a significant residual anisotropy in micelles when compared to the bare solvent confirms that C485 is localized in micelles.

Along similar lines, the fluorescence decay traces of C519$^-$ in water (490 nm), SDS (490 nm), Tx-100 (490 nm), and CTAB (470 nm) after excitation at 400 nm are shown in Figure 3A. The fluorescence lifetimes of C519$^-$ in different media are long and are dominated by the decay of the ICT state. As the fluorescence lifetimes are found to be greater than 1 ns (longer than the delay line of the upconversion setup), lifetime data was obtained from time-correlated single photon counting and is provided in Table 1 for C519$^-$ in different media. Important information about the localization of C519$^-$ in micelles can be obtained from the fluorescence anisotropy measurements. The anisotropy decay traces of C519$^-$ in different media are shown in Figure 3B. Here again, it is observed that the anisotropy decays of C519$^-$ in micelles follow biexponential decay function with a noticeable residual anisotropy when compared to water. These features confirm that C519$^-$ is localized in micelles. The exact location of the chromophore in micelles is very difficult to obtain from the anisotropy measurements. However, as observed in optical absorption and fluorescence measurements, C519$^-$ in CTAB offers different stabilization than that of SDS and Tx-100. This is ascribed to the

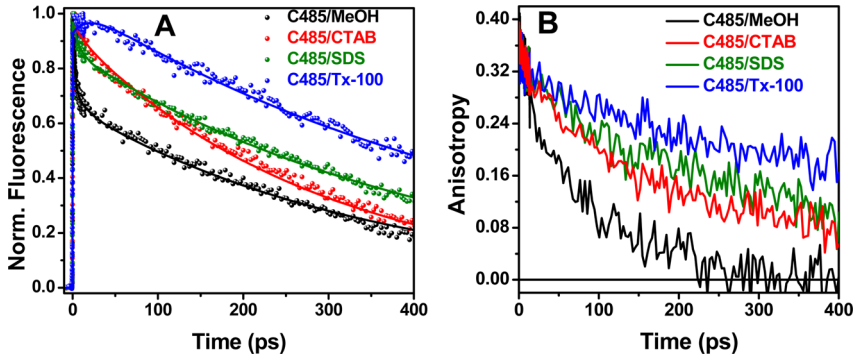

Figure 2. (A) Fluorescence kinetic decay traces of C485 in methanol (510 nm), SDS (510 nm), Tx-100 (500 nm), and CTAB (510 nm) after excitation at 400 nm. (B) Corresponding fluorescence anisotropy decay traces of C485 in different media.

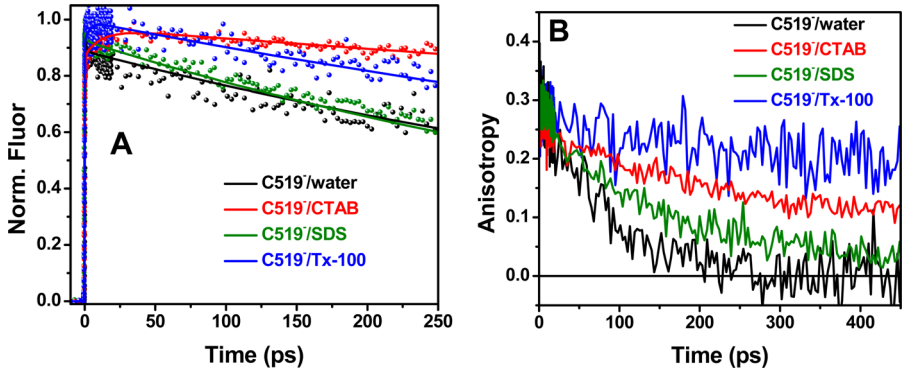

Figure 3. (A) Fluorescence kinetic decay traces of $C519^-$ in different micelles and corresponding fluorescence anisotropy decay traces (B).

electrostatic interaction between $C519^-$ and CTAB which is absent in other systems.

3.3. 2PA Measurements. As the central objective of the investigation is to study the 2PA properties of chromophores in micelles, TPEF measurements were performed to obtain the same.

3.3.1. 2PA Cross Sections of C485 in Different Media. Shown in Figure 4 are the 2PA cross sections of C485 in various media measured at different wavelengths. A closer look at the figure shows little variation in the 2PA cross sections of C485 in micelles and almost similar to that of methanol. Although C485 is localized in different regions of micelles with different micropolarities, the 2PA cross sections show minimal differences (Table 2). Several research groups have shown that the polarity effect on the 2PA cross sections of chromophores is rather nonmonotonic, and the present results on C485 show that the effect is minimal in microheterogeneous media as well.[45]

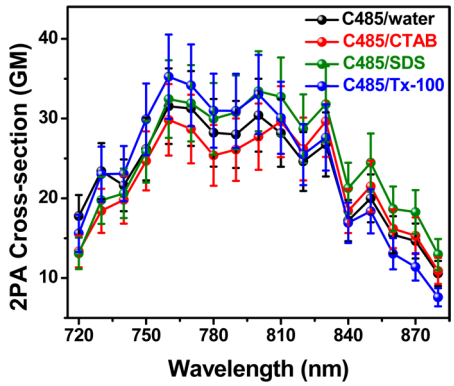

Figure 4. 2PA cross sections of C485 in water, SDS, CTAB, and Tx-100 at different wavelengths.

Table 2. Maximum 2PA Cross Sections of the Investigated Chromophores in Different Media

sample	$\eta\delta$	δ_{max} (GM)
C485/water	1.9	31 ± 5
C485/CTAB	2.6	29 ± 6
C485/SDS	5.3	33 ± 6
C485/Tx-100	11	35 ± 6
$C519^-$/water	35	50 ± 8
$C519^-$/CTAB	61.2	102 ± 16
$C519^-$/SDS	38.6	46 ± 8
$C519^-$/Tx-100	25.2	45 ± 8

3.3.2. 2PA Cross Sections of $C519^-$ in Different Media. The 2PA cross section trends of the anionic C519 are significantly different from that of the C485. Figure 5 and Table 2 show the 2PA cross sections of $C519^-$ in different micelles monitored at different wavelengths. The two-photon excitation spectra of $C519^-$ in different media shown in Figure 5 match the one-photon absorption for the most part except for a 10 nm shift to higher energies. Similar shift to higher energies is observed for the standard C485 in methanol.[56] Thus, the two-photon excitation observed in the study represents the lowest excited state of the chromophores. As the lowest excited state of coumarins has strong ICT character, both one- and two-photon excitation allow it. From Figure 5, it can be observed that $C519^-$ in water has a maximum 2PA cross section of 50 ± 8 GM in water and it is almost unchanged in SDS and Tx-100

dx.doi.org/10.1021/jp405416d | J. Phys. Chem. B 2013, 117, 10484−10491

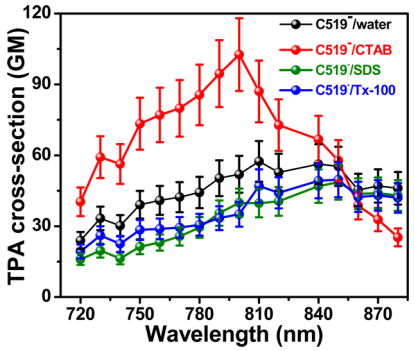

Figure 5. 2PA cross sections of C519⁻ in water, SDS, CTAB, and Tx-100 at different wavelengths.

which are anionic and neutral surfactants, respectively. In contrast, the maximum 2PA cross section of C519⁻ has increased to 102 ± 16 GM in CTAB (2-fold enhancement) and the 2PA excitation spectrum matched closely with the shift in absorption spectrum. The results show that the electrostatic interactions at the interface of the CTAB where the anionic chromophore is localized solubilized is probably the reason behind the 2PA cross-section enhancement.

However, it is necessary to understand if the enhancement is because of the organized assembly or the association of C519⁻ and CTAB surfactant.

3.3.3. 2PA Cross Sections as a Function of Surfactant Concentration. To answer the question if the enhancement is because of simple cation−anion interaction or due to the organized assembly of micelle, 2PA cross sections of C519⁻ were measured with increasing concentrations of CTAB. Shown in Figure 6 are the 2PA cross sections of C519⁻ with

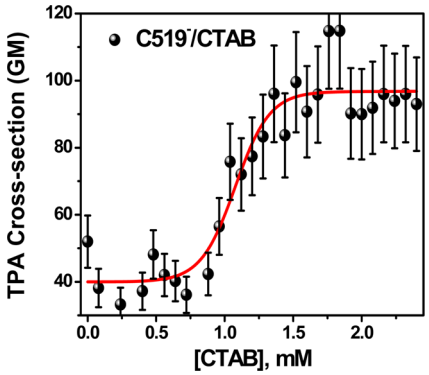

Figure 6. 2PA cross sections of C519⁻ with increasing concentrations of CTAB at 800 nm.

increasing concentrations of CTAB. It can be observed from the figure that the 2PA cross section of C519⁻ is unchanged until it reached a concentration of 0.8 mM of CTAB and showed 2 times enhancement after 1 mM. The cmc of CTAB is around 1 mM[61,62] and the results confirm that the enhancement of 2PA cross section is because of the organized micelle assembly and not due to cation−anion interaction between C519⁻ and CTAB. In addition, the absorption and fluorescence spectra of C519⁻ also shifted to higher energies at around cmc only (see Supporting Information). Preferential blue shift of absorption spectra of C519⁻ in CTAB micelle indicate that it is localized in an environment where the local electric fields (due to Stark shifts) are effective.

3.3.4. Mechanism of 2PA Enhancement. Three main observations are made from the 2PA cross sections of chromophores in different micellar media. First, the neutral C485 did not show significant change in 2PA cross sections in different micelles. Second, even the anionic C519 had shown little change in anionic SDS and neutral Tx-100. Finally, the anionic C519 had shown 200% enhancement when it is solubilized in the cationic CTAB. It is established in the literature that the local environments in micelles provide different micropolarities and microviscosities. It is also reported that the ionic micelles possess local electric fields at the headgroup of micelle/water interface.[57−63] There are four different regions in micelles, (i) Gouy−Chapman layer, region where the counterions reside; (ii) head group layer (Stern layer); (iii) palisade layer, region below the head group region where the hydration is observed; and (iv) core region, mostly hydrophobic region (Scheme 1).[64,65] The micropolarities and

Scheme 1. Cartoon Diagram Depicting the Possible Location of C519⁻ near the Head Group Region of CTAB

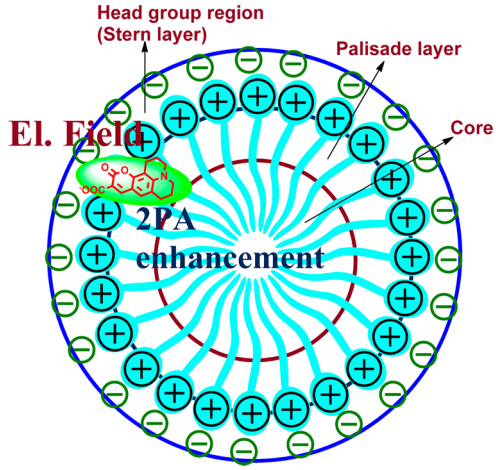

electric fields experienced by the chromophores in micelles are dependent on the location of the chromophore in the micellar environment. For instance, the highest local electric fields are expected and observed in the Stern layer region for ionic micelles.[66] However, palisade layer and core regions provide different environments with varying micropolarities.

Optical absorption and steady-state fluorescence measurements have shown that C485 is localized in the palisade layer of micelles but in different dielectric environments as evidenced from the differences in their fluorescence maxima. The fact that the 2PA cross sections are unchanged for C485 in different micelles indicates little influence of micropolarity on the two-photon properties of neutral C485. It has to be mentioned that the 2PA cross sections of C485 are similar in solvents of different polarity and is probably the reason behind the insensitivity to micropolarities. But, if a chromophore shows polarity-dependent 2PA cross sections, it can show differences in 2PA cross sections in different micelles as well. However, the 2PA cross sections of anionic C519 have shown an interesting 100% increase (i.e., ∼2 times) in 2PA cross section when it is solubilized in cationic CTAB while there is no change in other micellar systems. This result is again attributed to the location of C519⁻ in different micelles. Due to the electrostatic interactions, C519⁻ is expected to be solubilized in the Stern-layer region of CTAB while it resides away from the head group

dx.doi.org/10.1021/jp405416d | J. Phys. Chem. B 2013, 117, 10484−10491

region in other micelles (Scheme 1). Additional support for the location of C519$^-$ in CTAB comes from one-photon and two-photon fluorescence maxima as a function of CTAB concentration (see Supporting Information). Both one- and two-photon fluorescence maxima shifted to blue wavelength regions with micelle formation, indicating the influence of local electrostatic fields in the Stern layer on the optical properties of C519$^-$, which can be attributed to Stark shifts.[67]

Recently, Rebane and co-workers[68−70] have shown that the local electric fields can have marked influence on the 2PA cross sections with their work on fluorescent proteins.[68] The effect of local electric field on the 2PA cross sections of chromophores can be understood with the following expressions. In a sum-over-states formalism,[19,69] the two-state 2PA cross section ($\delta_{2-\text{state}}$) is given by

$$\delta_{2\text{-state}} = \frac{2(2\pi)^4 f_L^{\ 4}}{15(nhc)^2}(1 + 2\cos^2\theta)|\overrightarrow{M_{ge}}|^2|\overrightarrow{\Delta\mu_{ge}}|^2 g(2\nu) \quad (2)$$

where $\overrightarrow{M_{ge}}$ is the transition dipole moment vector between the ground state (g) and excited state (e), $\overrightarrow{\Delta\mu_{ge}}$ the difference between the permanent dipole moments in the ground and excited state, and θ is the angle between these two vectors. $g(2\nu)$ is the normalized line shape function, n is the refractive index, c is the speed of light, h is Planck's constant, and f_L is the local field factor (optical) given by $f_L = (n^2 + 2)/3$.

It can be seen that the 2PA cross section of the chromophore is proportional to the square of the change in dipole moment and change in permanent dipole moment. The local electric fields of an organized assembly contribute to change in dipole moment via an increase in induced dipole moment

$$\Delta\mu_{ge} = \Delta\mu_{ge}^0 + 0.5\Delta\mu_{ge}^{\text{ind}} = \Delta\mu_{ge}^0 + 0.5(\Delta\alpha)E \quad (3)$$

where $\Delta\mu_{ge}^0$ corresponds to the permanent dipole moment change in the zero-field situation, $\Delta\alpha = \alpha_e - \alpha_g$ is the change in polarizability between ground and excited states, and E is the local electric field. From the results of the 2PA enhancement, we have estimated the local electric field in the Stern layer of CTAB. $\Delta\mu_{ge}^0$ for C519$^-$ is determined from Lippert−Mataga plots[71−73] (see Supporting Information) and it was found to be around 5.2 D, and we have used the $\Delta\alpha$ for coumarins which is less than 10 ^{3} and close to 6 ^{3}.[74] From this data, the local electric field in the Stern-layer region of CTAB was estimated to be around 0.70 ± 0.3 MV/cm. The results discussed above have shown that the 2PA cross sections of chromophores can be enhanced if the chromophores are localized in the Stern layer of ionic micelles. This result is significant as the 2PA of appropriate chromophores can be used as markers of the electrostatic environments such as membranes, DNA, and proteins. Further work is ongoing in our laboratory to address the electric fields in several organized assemblies and confined geometries.

4. CONCLUSIONS

A systematic study of the 2PA cross sections of C485 and C519$^-$ in different micelle assemblies is reported. The results have shown that the 2PA cross sections of the neutral C485 are unchanged in different micellar environments. On the other hand, the 2PA cross sections of C519$^-$ have increased 2-fold when it was solubilized in the cationic CTAB micelle and are unchanged in anionic and neutral micelles. The enhancement in 2PA cross section for C519$^-$ in CTAB is attributed to the electrostatic fields that arose from the micelle assembly. Femtosecond fluorescence upconversion lifetimes and anisotropy measurements have shown that the chromophores are solubilized in the micelles. The titration measurements have shown that the 2PA cross sections are enhanced when the chromophore is present in the organized medium rather than simple anion−cation interactions. Local electric field in the head group region of CTAB was determined from the 2PA enhancement and it was found to be around 0.70 ± 0.30 MV/cm. The present study shows a new way to monitor the local electric fields in different organized and confined environments.

■ ASSOCIATED CONTENT

Supporting Information

The micropolarity calibration curve for C485, shift of C519$^-$ fluorescence maximum as a function of CTAB concentration, and Lippert−Mataga plot for C519$^-$ are provided. This material is available free of charge via the Internet at http://pubs.acs.org.

■ AUTHOR INFORMATION

Corresponding Author

*E-mail: rama.guda@wmich.edu.

Notes

The authors declare no competing financial interest.

■ ACKNOWLEDGMENTS

G.R. acknowledges the support of Western Michigan University-FRACAA and WMU start-up funds for the project. We also thank Ms Allison Renee Dubbink (Howard Hughes Medical Institute undergraduate student) for her work on the optical properties of C485 in different solvents.

■ REFERENCES

(1) Denk, W.; Strickler, J. H.; Webb, W. W. Two-Photon Laser Scanning Fluorescence Microscopy. *Science* **1990**, *248*, 73−76.

(2) Piston, D. W.; Masters, B. R.; Webb, W. W. Three-Dimensionally Resolved NAD(P)H Cellular Metabolic Redox Imaging of the in situ Cornea with Two-Photon Excitation Laser Scanning Microscopy. *J. Microsc.* **1995**, *178*, 20−27.

(3) Xu, C.; Zipfel, W.; Shear, J. B.; Wiliams, R. W.; Webb, W. W. Multiphoton Fluorescence Excitation: New Spectral Windows for Biological Nonlinear Microscopy. *Proc. Natl. Acad. Sci. U.S.A.* **1996**, *93*, 10763−10768.

(4) Wei, P.; Tan, O. F.; Zhu, Y.; Duan, G. H. Axial Super Resolution of Two-Photon Microfabrication. *Appl. Opt.* **2007**, *46*, 3694−3699.

(5) Leatherdale, C. A.; DeVoe, R. J. Two-Photon Microfabrication using Two-Component Photoinitiation Systems: Effect of Photosensitizer and Acceptor Concentrations. *Proc. SPIE* **2003**, *5211*, 112−123.

(6) Teh, W. H.; Durig, U.; Salis, G.; Harbers, R.; Drechsler, U.; Mahrt, R. F.; Smith, C. G.; Guntherodt, H. SU-8 for Real Three-Dimensional Subdiffraction-limit Two-Photon Microfabrication. *Appl. Phys. Lett.* **2004**, *84*, 4095−4097.

(7) Parthenopoulos, D. A.; Rentzepis, P. M. Two-Photon Volume Information Storage in Doped Polymer Systems. *J. Appl. Phys.* **1990**, *68*, 5814−5818.

(8) He, G. S.; Gvishi, R.; Prasad, P. N.; Reinhardt, B. A. Two-Photon Absorption based Optical Limiting and Stabilization in Organic Molecule-doped Solid Materials. *Opt. Commun.* **1995**, *117*, 133−136.

(9) He, G. S.; Xu, G. C.; Prasad, P. N.; Reinhardt, B. A.; Bhatt, J. C.; Dillard, A. G. Two-Photon Absorption and Optical-Limiting Properties of Novel Organic Compounds. *Opt. Lett.* **1995**, *20*, 435−437.

(10) He, G. S.; Bhawalkar, J. D.; Zhao, C.; Prasad, P. N. Optical Limiting Effect in a Two-Photon Absorption Dye Doped Solid Matrix. *Appl. Phys. Lett.* **1995**, *67*, 2433−2435.
(11) Zhao, P. D.; Chen, P.; Tang, G. Q.; Zhang, G. L.; Chen, W. Two-Photon Spectroscopic Properties of a New Chlorin Derivative Photosensitizer. *Chem. Phys. Lett.* **2004**, *390*, 41−44.
(12) Fisher, W. G.; Partridge, W. P.; Dees, C.; Wachter, E. A. Simultaneous Two-Photon Activation of Type-I Photodynamic Therapy Agents. *Photochem. Photobiol.* **1997**, *66*, 141−155.
(13) Fabbrni, G.; Riccó, R.; Menna, E.; Maggini, M.; Amendola, V.; Garbin, M.; Villano, M.; Meneghetti, M. Sequential Multiphoton Absorption Enhancement Induced by Zinc Complexation in Functionalized Distyrylbenzene Analogs. *Phys. Chem. Chem. Phys.* **2007**, *9*, 616−621.
(14) Bhaskar, A.; Ramakrishna, G.; Tweig, R. J.; Goodson, T., III Zinc Sensing via Enhancement of Two-Photon Excited Fluorescence. *J. Phys. Chem. C* **2007**, *111*, 14607−14610.
(15) Weerasinghe, A.; Schmeising, C.; Varaganti, S.; Ramakrishna, G.; Sinn, E. Single- and Multiphoton Turn-On Fluorescent Fe^{3+} Sensors Based on Bis(rhodamine). *J. Phys. Chem. B* **2010**, *114*, 9413−9419.
(16) Wang, Y.; Goodson, T., III Early Aggregation in Prion Peptide Nanostructures Investigated by Nonlinear and Ultrafast Time-Resolved Fluorescence Spectroscopy. *J. Phys. Chem. B* **2007**, *111*, 327−330.
(17) Cotlet, M.; Goodwin, P. M.; Waldo, G. S.; Werner, J. H. A Comparison of the Fluorescence Dynamics of Single Molecules of a Green Fluorescent Protein: One- versus Two-Photon Excitation. *Chem. Phys. Chem.* **2006**, *7*, 250−260.
(18) Kannan, R.; Chung, S.; Lin, T.; Prasad, P. N.; Vaia, R. A.; Tan, L. Toward Highly Active Two-Photon Absorbing Liquids. Synthesis and Characterization of 1,3,5-Triazine-Based Octupolar Molecules. *Chem. Mater.* **2004**, *16*, 185−195.
(19) Beljonne, D.; Wenseleers, W.; Zojer, E.; Shuai, Z.; Vogel, H.; Pond, S. J. K.; Perry, J. W.; Marder, S. R.; Bredas, J.-L. Role of Dimensionality on the Two-photon Absorption Response of Conjugated Molecules: The Case of Octupolar Compounds. *Adv. Funct. Mater.* **2002**, *12*, 631−641.
(20) Chung, S.-J.; Kim, K.-S.; Lin, T.-C.; He, G. C.; Swiatkiewicz, J.; Prasad, P. N. Cooperative Enhancement of Two-Photon Absorption in Multi-branched Structures. *J. Phys. Chem. B* **1999**, *103*, 10741−10745.
(21) Bhaskar, A.; Ramakrishna, G.; Lu, Z. K.; Twieg, R.; Hales, J. M.; Hagan, D. J.; Van Stryland, E.; Goodson, T. Investigation of Two-Photon Absorption Properties in Branched Alkene and Alkyne Chromophores. *J. Am. Chem. Soc.* **2006**, *128*, 11840−11849.
(22) Kim, H. M.; Cho, B. R. Two-Photon Materials with Large Two-Photon Cross Sections. Structure-Property Relationship. *Chem. Commun.* **2009**, 153−164.
(23) Albota, M.; Beljonne, D.; Bredas, J.-L.; Ehrlich, J. E.; Fu, J.-Y.; Heikal, A. A.; Hess, S. E.; Kogej, T.; Levin, M. D.; Marder, S. R.; et al. Design of Organic Molecules with Large Two-Photon Absorption Cross Sections. *Science* **1998**, *281*, 1653−1656.
(24) Drobizhev, M.; Karotki, A.; Dzenis, Y.; Rebane, A.; Suo, Z.; Spangler, C. W. Strong Cooperative Enhancement of Two-Photon Absorption in Dendrimers. *J. Phys. Chem. B* **2003**, *107*, 7540−7543.
(25) Charlot, M.; Izard, N.; Mongin, O.; Riehl, D.; Blanchard-Desce, M. Optical Limiting with Soluble Two-Photon Absorbing Quadrupoles: Structure−Property Relationships. *Chem. Phys. Lett.* **2006**, *417*, 297−302.
(26) Dhenadhayalan, N.; Selvaraju, C. Role of Photoionization on the Dynamics and Mechanism of Photoinduced Electron Transfer Reaction of Coumarin 307 in Micelles. *J. Phys. Chem. B* **2012**, *116*, 4908−4920.
(27) Faeder, J.; Ladanyi, B. M. Solvation Dynamics in Reverse Micelles: The Role of Headgroup-Solute Interactions. *J. Phys. Chem. B* **2005**, *109*, 6732−6740.
(28) Tamoto, Y.; Segawa, H.; Shirota, H. Solvation Dynamics in Aqueous Anionic and Cationic Micelle Solutions: Sodium Alkyl Sulfate and Alkyltrimethylammonium Bromide. *Langmuir* **2005**, *21*, 3757−3764.
(29) Dutt, G. B. Are the Experimentally Determined Microviscosities of the Micelles Probe Dependent? *J. Phys. Chem. B* **2004**, *108*, 3651−3657.
(30) Hazra, P.; Chakrabarty, D.; Chakraborty, A.; Sarkar, N. Solvation Dynamics of Coumarin 480 in Neutral (TX-100), Anionic (SDS), and Cationic (CTAB) Water-in-oil Microemulsions. *Chem. Phys. Lett.* **2003**, *382*, 71−80.
(31) Mohanty, J.; Nau, W. M. Ultrastable Rhodamine with Cucurbituril. *Angew. Chem. Int. Ed.* **2005**, *44*, 3750−3754.
(32) Bhasikuttan, A. C.; Mohanty, J.; Nau, W. M.; Pal, H. Efficient Fluorescence Enhancement and Cooperative Binding of an Organic Dye in a Supra-Biomolecular Host-Protein Assembly. *Angew. Chem. Int. Ed.* **2007**, *46*, 4120−4122.
(33) Barooah, N.; Mohanty, J.; Pal, H.; Bhasikuttan, A. C. Non-Covalent Interactions of Coumarin Dyes with Cucurbit(7)uril Macrocycle: Modulation of ICT to TICT Conversion. *Org. Biomol. Chem.* **2012**, *10*, 5055−5062.
(34) Singh, A. K.; Mondal, J. A.; Ramakrishna, G.; Ghosh, H. N.; Bandyopadhyay, T.; Palit, D. K. Ultrafast Dynamics of Photoinduced Intermolecular Electron Transfer Process in Micelle. *J. Phys. Chem. B* **2005**, *109*, 4014−4023.
(35) Prazeres, T. J.; Beija, M.; Fernandes, F. V.; Marcelino, P. G.; Farinha, J. P.; Martinho, J. M. Determination of the Critical Micelle Concentration of Surfactants and Amphiphilic Block Copolymers using Coumarin 153. *Inorg. Chim. Acta* **2012**, *381*, 181−187.
(36) Mali, K. S.; Dutt, G. B.; Mukherjee, T. Photoisomerization of a Carboxyanine Derivative in Reverse Phases of a Block Copolymer: Evidence for the Existence of Water Droplets. *Langmuir* **2007**, *23*, 1041−1046.
(37) Tan, Y.; Zhang, Q.; Yu, J.; Zhao, X.; Tian, Y.; Cui, Y.; Hao, X.; Yang, Y.; Qian, G. Solvent Effect on Two-Photon Absorption (TPA) of Three Novel Dyes with Large TPA Cross-section and Red Emission. *Dyes Pigm.* **2013**, *97*, 58−64.
(38) Zhao, Y.; Ren, A.-M.; Feng, J.-K.; Zhou, X.; Ai, X.-C.; Su, W.-J. Theoretical Study of Solvent Effect on One and Two-Photon Absorption Properties of Starburst DCM Derivatives. *Phys. Chem. Chem. Phys.* **2009**, *11*, 11538−11545.
(39) Young, H. Y.; Liu, B.; Kohler, B.; Korystov, D.; Mikhailovsky, A.; Bazan, G. C. Solvent Effects on the Two-Photon Absorption of Distyrylbenzene Chromophores. *J. Am. Chem. Soc.* **2005**, *127*, 14721−14729.
(40) Zhou, Y.; Miao, Q.; Sun, Y.; Gel'mukhanov, F.; Wang, C. Solvent Effect on Dynamical TPA and Optical Limiting of BDMAS Molecular Media for Nanosecond and Femtosecond Laser Pulses. *J. Phys. B: At. Mol. Opt. Phys.* **2011**, *44*, 1−7.
(41) Zhao, K.; Ferrighi, L.; Frediani, L.; Wang, C.; Luo, Yi. Solvent Effects on Two-Photon Absorption of Dialkylamino Substituted Distyrylbenzene Chromophore. *J. Chem. Phys.* **2007**, *126*, 204509−204514.
(42) Wielgus, M.; Bartkowiak, W.; Samoc, M. Two-Photon Solvatochromism. I. Solvent Effects on Two-Photon Absorption Cross-section of 4-dimethylamino-nitrostilbene (DANS). *Chem. Phys. Lett.* **2012**, *554*, 113−116.
(43) Wang, H.; Li, Z.; Shao, P.; Qin, J.; Huang, Z. Two-Photon Absorption Property of a Conjugated Polymer: Influence of Solvent and Concentration on Its Property. *J. Phys. Chem. B* **2010**, *114*, 22−27.
(44) Alam, M.; Chattopadhyaya, M.; Chakrabarti, S.; Ruud, K. High-polarity Solvents Decreasing the Two-Photon Transition Probability of Through-Space Charge-Transfer Systems—A Surprising In Silico Observation. *J. Phys. Chem. Lett.* **2012**, *3*, 961−966.
(45) Murugan, N. A.; Chakrabarti, S.; Ågren, H. Solvent Dependence of Structure, Charge Distribution, and Absorption Spectrum in the Photochromic Merocyanine Spiropyran Pair. *J. Phys. Chem. B* **2011**, *115*, 4025−4032.
(46) Leng, W.; Bazan, G. C.; Kelly, A. M. Solvent effects on Resonance Raman and Hyper-Raman Scatterings for a Centrosym-

metric Distyrylbenzene and Relationship to Two-Photon Absorption. *J. Chem. Phys.* **2009**, *130*, 044501−08.
(47) Woo, H. Y.; Korystov, D.; Mikhailovsky, A.; Nguyen, T.; Bazan, G. C. Two-Photon Absorption in Aqueous Micellar Solutions. *J. Am. Chem. Soc.* **2005**, *127*, 13794−13795.
(48) Fang, Z.; Zhang, X.; Laic, Y. H.; Liu, B. Bridged Triphenylamine Based Molecules with Large Two-Photon Absorption Cross Sections in Organic and Aqueous Media. *Chem. Commun.* **2009**, 920−922.
(49) Chen, C.; Tian, Y.; Cheng, Y.; Young, A. C.; Ka, J.; Jen, A. K. Two-Photon Absorbing Block Copolymer as a Nanocarrier for Porphyrin: Energy Transfer and Singlet Oxygen Generation in Micellar Aqueous Solution. *J. Am. Chem. Soc.* **2007**, *129*, 7220−7221.
(50) Woo, H. Y.; Hong, J. W.; Liu, B.; Mikhailovsky, A.; Korystov, D.; Bazan, G. C. Water-Soluble [2.2] Paracyclophane Chromophores with Large Two-Photon Action Cross Sections. *J. Am. Chem. Soc.* **2005**, *127*, 820−821.
(51) Nag, O. K.; Lim, C. S.; Nguyen, B. L.; Kim, B.; Jang, J.; Han, J. H.; Cho, B. R.; Woo, H. Y. pH-responsive Water Soluble Smart Vesicles Containing a bis(styryl)benzene Derivative for Two-Photon Microscopy Imaging. *J. Mater. Chem.* **2012**, *22*, 1977−1984.
(52) Nag, O. K.; Nayak, R. R.; Lim, C. S.; Kim, I. H.; Kyhm, K.; Cho, B. R.; Woo, H. Y. Two-Photon Absorption Properties of Cationic 1,4-Bis(styryl) benzene Derivatives and Its Inclusion Complexes with Cyclodextrins. *J. Phys. Chem. B* **2010**, *114*, 9684−9690.
(53) Willard, D. M.; Riter, R. E.; Levinger, N. E. Dynamics of Polar Solvation in Lecithin/Water/Cyclohexane Reverse Micelles. *J. Am. Chem. Soc.* **1998**, *120*, 4151−4160.
(54) Kahlow, M. A.; Jarzeba, W.; Kang, T. J.; Barbara, P. F. Femtosecond Resolved Solvation Dynamics in Polar Solvents. *J. Chem. Phys.* **1989**, *90*, 151−158.
(55) Xu, C.; Webb, W. W. Measurement of Two-Photon Excitation Cross Sections of Molecular Fluorophores with Data from 690 to 1050 nm. *J. Opt. Soc. Am. B* **1996**, *13*, 481−491.
(56) Makarov, N. S; Dorbizhev, M.; Rebance, A. Two-Photon Absorption Standards in the 550−1600 nm Excitation Wavelength Range. *Opt. Exp.* **2008**, *6*, 4029−4047.
(57) Varaganti, S.; Ramakrishna, G. Dynamics of Interfacial Charge-Transfer Emission in Small Molecule-Sensitized TiO_2 Nanoparticles: Is it Localized or Delocalized? *J. Phys. Chem. C* **2010**, *114*, 13917−13925.
(58) Lakowicz, J. R. *Principles of Fluorescence Spectroscopy*, 2nd ed.; Kluwer Academic/Plenum Publisher: New York, 1999.
(59) Nad, S.; Kumbhakar, M.; Pal, H. Photophysical Properties of Coumarin-152 and Coumarin-481 Dyes: Unusual Behavior in Nonpolar and in Higher Polarity Solvents. *J. Phys. Chem. A* **2003**, *107*, 4808−4816.
(60) Maiti, N. C.; Krishna, M. M. G.; Britto, P. J.; Periasamy, N. Fluorescence Dynamics of Dye Probes in Micelles. *J. Phys. Chem. B* **1997**, *101*, 11051−11060.
(61) Yusof, N. S. M.; Khan, M. N.; Ashokkumar, M. Characterization of the Structural Transitions in CTAB Micelles Using Fluorescein Isothiocyanate. *J. Phys. Chem. C* **2012**, *116*, 15019−15027.
(62) Halder, M. Determination of the Critical Micellar Concentration (CMC) of a Cationic Micelles from Stokes Shift Data. *Chem. Educ.* **2007**, *12*, 33−36.
(63) Fendler, J. H. *Membrane Mimetic Chemistry*; Wiley: New York, 1982.
(64) Rosen, J. M. *Surfactants and Interfacial Phenomena*; John Wiley Sons: New York, 1978.
(65) Stigler, D. Micelle Formation by Ionic Surfactants III Model of Stern Layer, Ion distribution and Potential Fluctuations. *J. Phys. Chem.* **1975**, *79*, 1008−1014.
(66) Jiang, Y.-B.; Wang, X.-J.; Jin, M.-G.; Lin, L.-R. The effect of Micelle-Water Interface Electric Field on the Intramolecular Charge Transfer within Ionic Micelle: Dual Fluorescence of Sodium p-dialkylaminobenzoate in Cetyltrimethylammonium Micelles. *J. Photochem. Photobiol. A: Chem.* **1999**, *126*, 125−133.
(67) Samanta, A.; Paul, B. K.; Guchchait, N. Studies of Bio-Mimetic Medium of Ionic and Non-Ionic Micelles by Simple Charge Transfer Probe N, N-dimethylamino naphthyl-(acrylo)-nitrate. *Spectrochim. Acta Part A: Mol. Biomol. Spectrosc.* **2011**, *78*, 1525−1534.
(68) Dorbizhev, M.; Makarov, N. S.; Tillo, S. E.; Hughes, T. E.; Rebane, A. Two-Photon Absorption Properties of Fluorescent Proteins. *Nature Methods* **2011**, *8*, 393−399.
(69) Drobizhev, M.; Tillo, S.; Makarov, N. S.; Hughes, T. E.; Rebane, A. Color Hues in Red Fluorescent Proteins are due to Internal Quadratic Stark Effect. *J. Phys. Chem. B* **2009**, *113*, 12860−12864.
(70) Rebane, A.; Drobizhev, M.; Makarov, N. S.; Beurman, E.; Tillo, S.; Hughes, T. New All-Optical Method for Measuring Molecular Permanent Dipole Moment Difference using Two-Photon Absorption Spectroscopy. *J. Lumin.* **2010**, *130*, 1619−1623.
(71) Lippert, E. Dipolmoment und Elektronenstruktur von angeregten Molekülen. *Z. Naturforsch., A: Phys. Sci.* **1955**, *10*, 541−545.
(72) Mataga, N.; Kaifu, Y.; Koizumi, M. The Solvent Effect on Fluorescence Spectrum − Change of Solute-Solvent Interaction during the Lifetime of Excited Solute Molecule. *Bull. Chem. Soc. Jpn.* **1955**, *28*, 690−691.
(73) Mataga, N.; Kaifu, Y.; Koizumi, M. Solvent Effects upon Fluorescence Spectra and the Dipole Moments of Excited Molecules. *Bull. Chem. Soc. Jpn.* **1956**, *29*, 465−470.
(74) Chowdhury, A.; Locknar, S. A.; Premvardhan, L. L.; Peteanu, L. A. Effects of Matrix Temperature and Rigidity on the Electronic Properties of Solvatochromic Molecules: Electroabsorption of Coumarin 153. *J. Phys. Chem. A* **1999**, *103*, 9615−9625.